

Magnetic separation of pentlandite from serpentine by selective magnetic coating

Ji-wei Lu^{1,3)}, Zhi-tao Yuan¹⁾, Xiao-fei Guo²⁾, Zhong-yun Tong¹⁾, and Li-xia Li¹⁾

1) School of Resources and Civil Engineering, Northeastern University, Shenyang 110819, China

2) School of Mining Engineering, University of Science and Technology Liaoning, Anshan 114051, China

3) Shaanxi Key Laboratory for the Comprehensive Utilization of Tailings Resources, Shangluo University, Shangluo 726000, China

(Received: 26 February 2018; revised: 27 June 2018; accepted: 6 August 2018)

Abstract: In this study, pentlandite was selectively separated from serpentine using magnetic coating technology by adjusting and optimizing pH, stirring speeds, magnetic field intensities, and dosages of sodium hexametaphosphate (SHMP) and sodium oleate (SO). A magnetic concentrate with Ni grade of 20.8% and Ni recovery of 80.5% was attained under the optimized operating conditions. Considering the above, the adsorption behaviors of SHMP and SO and the surface properties of minerals after the magnetic coating were studied by Fourier transform infrared (FTIR) spectroscopy, X-ray diffraction (XRD), and scanning electron microscopy (SEM). The results show that magnetite was preferentially coated on the pentlandite surfaces and sparingly coated on the serpentine surfaces in the presence of SHMP and SO. Furthermore, calculations by Derjaguin-Landau-Verwey-Overbeek (DLVO) theory indicate that the preferential adsorption of magnetite on the pentlandite surfaces is due to the presence of a hydrophobic interaction between the magnetite and pentlandite, which is much stronger than the interaction between magnetite and serpentine.

Keywords: dispersant; coagulant; magnetic coating; magnetic separation; hydrophobic interaction

1. Introduction

The separation of pentlandite from magnesium silicate gangue minerals (i.e., serpentine) is a worldwide challenging issue in the processing of sulfide nickel-copper ores. The magnesium silicate of serpentine mainly causes high pulp viscosity and slime coating on the surfaces of pentlandite to interfere with its flotation [1–2]; therefore, it is easily floated into the nickel concentrate, thereby reducing Ni recovery and grade. This seriously affects the following smelting process [3–4]. In such condition, addition of depressants or dispersants such as sodium silicate, sodium hexametaphosphate (SHMP), and carboxymethyl cellulose is a universal, effective, and inexpensive method for the desorption of serpentine from pentlandite surfaces. However, dispersants are rarely used because of the poor desorption in actual concentrators. Therefore, we propose a magnetic coating technology to separate pentlandite from serpentine by magnetic separation, which is different from the tradi-

tional froth flotation.

The separation of different minerals using selective magnetic coating by the addition of fine magnetic seeds to enhance the magnetism of target minerals has been described both theoretically and experimentally by different scholars [5–7]. Meanwhile, in our previous work on magnetic separation of pentlandite from serpentine using magnetic coating technology, we found that magnetite could be coated on the pentlandite surfaces, and pentlandite recovery significantly increased with increase in the amount of magnetite. The effect of magnetite on magnetic coating behaviors between pentlandite and serpentine was discussed in detail, but the effects of SHMP and sodium oleate (SO) reagents on magnetic coating behaviors in the pentlandite and serpentine system were not discussed. Furthermore, other factors (e.g., slurry pH, magnetic field intensity, and stirring intensity) that affected the magnetic coating of magnetite on the pentlandite surface were also not well surveyed. Therefore, based on our previous success of separating pentlandite

from serpentine via magnetic coating technology, the objective of this work is to further study the effects of various factors on the magnetic coating of magnetite in a pentlandite and serpentine system to better understand the magnetic coating process, especially the role of SHMP and SO surfactants, through Fourier transform infrared spectroscopy (FTIR), X-ray diffraction (XRD), scanning electron microscopy (SEM), and Derjaguin-Landau-Verwey-Overbeek (DLVO) theory.

2. Experimental

2.1. Materials

Pentlandite (Fig. 1(a)), serpentine (Fig. 1(b)), and magnetite (Fig. 1(c)) were obtained from Jinchuan, Xiuyan, and Nanfen, respectively, in China. X-ray diffraction and chemical multi-element analyses of each mineral confirmed that they were all of high purity with small amounts of pyrite in pentlandite samples and trace amounts of quartz in magnetite samples, respectively [8]. Scanning electron microscopy images and energy dispersive spectroscopy (EDS) patterns further confirmed that each mineral was almost free of impurities as shown in Fig. 1. Furthermore, the particle size of magnetite was extremely fine, below 5 μm (Fig. 1(c)). In addition, pentlandite was ground to a particle size below 74 μm (according to the industrial process of Jinchuan Group Co., Ltd., China) using a conical ball mill (Wuhan Exploration Machinery Factory, China, model XMQ $\phi 240 \text{ mm} \times 90 \text{ mm}$). Serpentine was ground using a ceramic ball mill (Wuhan Exploration Machinery Factory, China, model XMCQ $\phi 180 \text{ mm} \times 200 \text{ mm}$) to less than 45 μm . The median diameters D_{50} of the pentlandite and serpentine were 16.66 and 12.88 μm , respectively, measured by a Malvern laser particle size analyzer, model 2000, and the results are shown in Fig. 2.

tion Machinery Factory, China, model XMQ $\phi 240 \text{ mm} \times 90 \text{ mm}$). Serpentine was ground using a ceramic ball mill (Wuhan Exploration Machinery Factory, China, model XMCQ $\phi 180 \text{ mm} \times 200 \text{ mm}$) to less than 45 μm . The median diameters D_{50} of the pentlandite and serpentine were 16.66 and 12.88 μm , respectively, measured by a Malvern laser particle size analyzer, model 2000, and the results are shown in Fig. 2.

2.2. Reagents

Sodium hexametaphosphate ($(\text{NaPO}_3)_6$) and SO ($\text{C}_{18}\text{H}_{33}\text{NaO}_2$), both purchased from Tianjin Kermil Inc., were used as the dispersant and coagulant, respectively, while HCl and NaOH (Tianjin Kermil Inc.) were used as pH modifiers. All reagents described above were of analytical grade.

2.3. Magnetic coating and magnetic separation tests

An inflatable hanging slot flotation machine (Jilin Exploration Machinery Factory, China, model XFGC_{III}, 200 mL cell) was used to conduct magnetic coating tests, which has been usually employed in flotation studies [9–11]. After the magnetic coating was realized, the coated suspension was separated by a wet magnetic separator (XCSQ-50 \times 70, Wuhan, China). Magnetic separation was carried out by varying the pH and magnetic field intensities. More detailed descriptions have been shown in earlier publications [8,12].

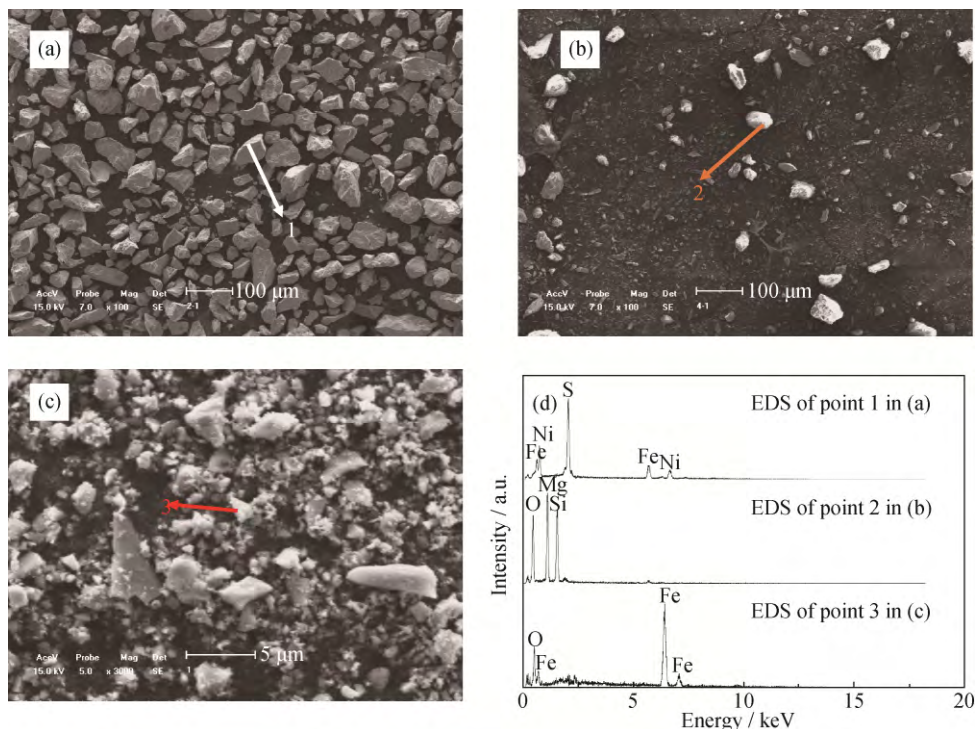


Fig. 1. SEM images of pentlandite (a), serpentine (b), and magnetite (c) and EDS patterns (d).

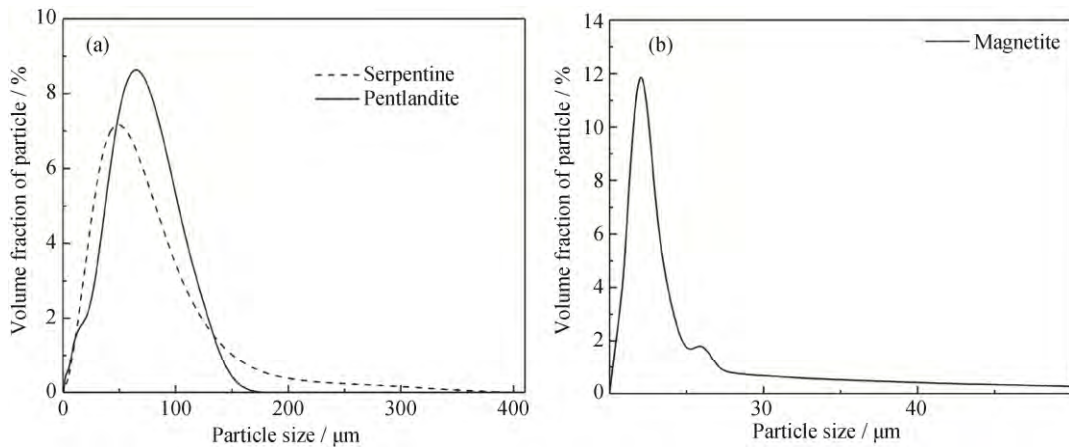


Fig. 2. Particle size distribution of pentlandite and serpentine (a) and magnetite (b).

2.4. FTIR study

The infrared spectra of mineral samples with and without reagents were analyzed using an FTIR spectrometer (FTIR, Model 380, Thermo Nicolet Co., USA). Disks were prepared by mixing approximately 2 mg of the desired sample and 200 mg of spectroscopic grade KBr for the following FTIR studies.

2.5. XRD and SEM studies

The magnetic concentrate obtained by magnetic separation was analyzed using XRD on an X-ray diffractometer (PW3040/60, Philips, Netherlands) with graphite monochromatized Cu $\text{K}\alpha$ radiation operating at 40 kV and 30 mA at room temperature. The analysis was conducted through a 2θ range from 10° to 90° .

The image and composition of different mineral grains were determined using a scanning electron microscope (Hitachi, S-3400N, Japan) with an energy dispersive X-ray spectrometer (Hitachi, Japan). The SEM images produced by the secondary or backscattered electrons were used to map the surface topographies. Energy dispersive spectrometry was used for elemental identification on the surface particles of interest.

Note that the non-coating magnetite fines in magnetic concentrates were removed by a hand-held magnet before the FTIR and XRD measurements.

3. Results and discussion

3.1. Results of magnetic coating of single minerals

To determine the suitable pH range and reagent system for the separation of pentlandite from serpentine, the effects of pH, SHMP as a dispersant, and SO as a coagulant on the magnetic coating of magnetite on pentlandite and serpentine

were studied. The results are presented in Figs. 3–5. The impeller rotation speed was set at $2400 \text{ r}\cdot\text{min}^{-1}$ and magnetic field intensity was set to 0.25 T. No reagent was added besides magnetite of 4wt% for the pH experiments.

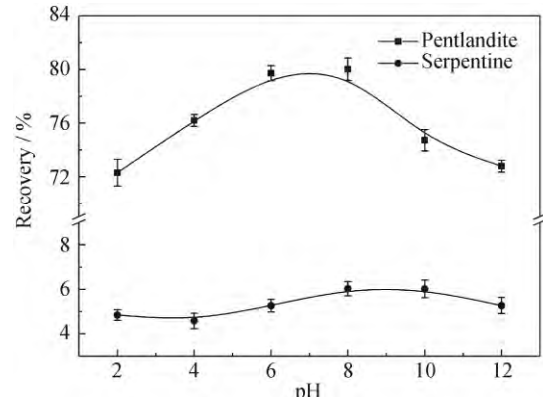


Fig. 3. Effect of pH on serpentine and pentlandite recoveries.

As shown in Fig. 3, the coating of magnetite on the serpentine and pentlandite surfaces was sensitive to pH values. The coating of magnetite on serpentine increased with the increase in pH between 4 and 10. Under the strong acidic and alkaline pH conditions, the magnetite coating for both serpentine and pentlandite particles was very weak. Although the magnetic coating on the serpentine surface began to occur at pH 6.0, the serpentine recovery was still very low. The maximum coating was obtained under a pH of around 8.0, and the recovery of serpentine was only 6.03%, which clearly indicates that it was very difficult for magnetite fines to be coated on the serpentine surface. A similar trend was also observed in the magnetic coating of magnetite on pentlandite surfaces, but the coating was much more sensitive to pH values. With increase in the pH values, the pentlandite recovery increased markedly within a pH range of 2–8 with the recoveries ranging from 72.1% to 79.9%. Above pH 8.0,

the recovery of pentlandite began to drop, and the stronger the alkaline, the more the decline because of the production of strong electrostatic repulsion between the magnetite and pentlandite particles possibly due to similar negative surface charges (surface potentials) at alkaline pH conditions [13]. Furthermore, the recovery of pentlandite appeared to be more efficient at a neutral pH range of 4–8 with the maximum recovery of around 80%. Considering the operability of magnetic separation, the selective coating of magnetite on the pentlandite surface was determined to be at the natural pH of 6.8–7.2.

From the results in Fig. 4, the addition of a dispersant is needed to weaken the coating of magnetite on serpentine. An increase in SHMP concentration resulted in a decrease in the serpentine recovery (Fig. 4). The best dosage range was between 20 and 60 mg·L⁻¹. When the SHMP concentration was more than 40 mg·L⁻¹, the serpentine recovery slightly decreased, and nearly leveled off after 60 mg·L⁻¹. The serpentine recovery decreased from 5.6% to about 4.0%. As a result, 40 mg·L⁻¹ of SHMP was adopted in the following magnetic coating tests. However, under such circumstance, the pentlandite recovery also decreased slightly from about 80% to about 78%. Therefore, a coagulant is necessary to strengthen the selective coating of magnetite on pentlandite particles.

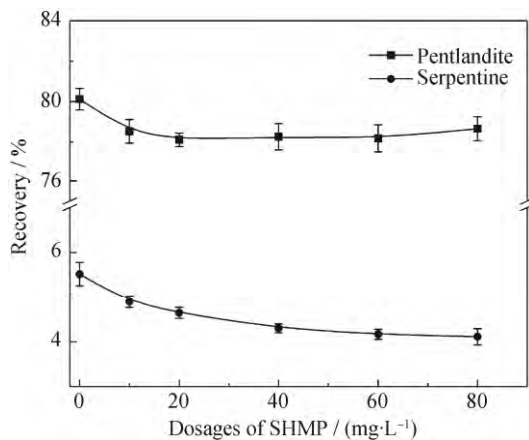


Fig. 4. Effect of SHMP on serpentine and pentlandite recoveries.

The pentlandite recovery significantly increased from 80% to around 95% with increase in the SO dosage to 400 mg·L⁻¹ (Fig. 5). With further increase in SO concentration, the pentlandite recovery increased only slightly. Hence, SO concentration of 400 mg·L⁻¹ was chosen for the following magnetic coating tests. However, the serpentine recovery increased only from 5.4% to 7.2%, and the increasing trend seemed likely to continue if the coagulant dosage was continually increased. The SHMP dispersant is indeed needed

for dispersing serpentine and magnetite particles (comparing the recovery without SHMP and that with 40 mg·L⁻¹ SHMP, the recovery decreased from 8.1% to 7.2%).

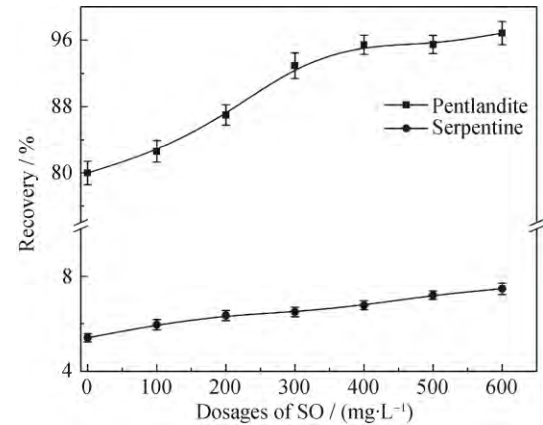


Fig. 5. Effect of SO on serpentine and pentlandite recoveries.

3.2. Results of magnetic coating of mixed minerals

The above analyses indicate that the fine magnetite particles selectively coated the pentlandite surface. In contrast, the magnetite particles coated the serpentine surface only sparingly; thus, pentlandite can be separated from serpentine using magnetic coating technology. On the basis of the above observations and results, magnetic coating tests on an artificial mineral mixture were performed to investigate the effect of SHMP and SO reagents on the separation of the pentlandite-serpentine mixtures (pentlandite to serpentine ratio was 1:2). The results are presented in Fig. 6.

From Fig. 6(a), the Ni grade increased with the increase in the SHMP dosage, while the Ni recovery decreased gradually; this can be mainly attributed to the dispersion effect of SHMP on the pentlandite and magnetite particles. Above all, with the addition of SHMP and the increase in its dosages, the grade and recovery of MgO both decreased. The grade decreased from about 4.0% to about 3.0%, and the recovery decreased from 6.2% to 4.5%. This suggests that serpentine minerals were well dispersed by the addition of SHMP, and according to the results in Fig. 6(a), the optimal SHMP dosage for minerals dispersion was found to be 60 mg·L⁻¹. An increase in the SO dosage resulted in an increase in Ni recovery (Fig. 6(b)), and at the same time, there was a slight drop in Ni grade. This may be because SO greatly improved the coating of magnetite fines on the pentlandite surfaces to increase the recovery; in addition, SO also favored the adhesion of magnetite fines to serpentine particles, which were also collected by magnetic separation, and led to the decline of the Ni grade. Therefore, the

grade and recovery of MgO also increased with increasing SO dosages (Fig. 6(b)). Thus, considering the indexes

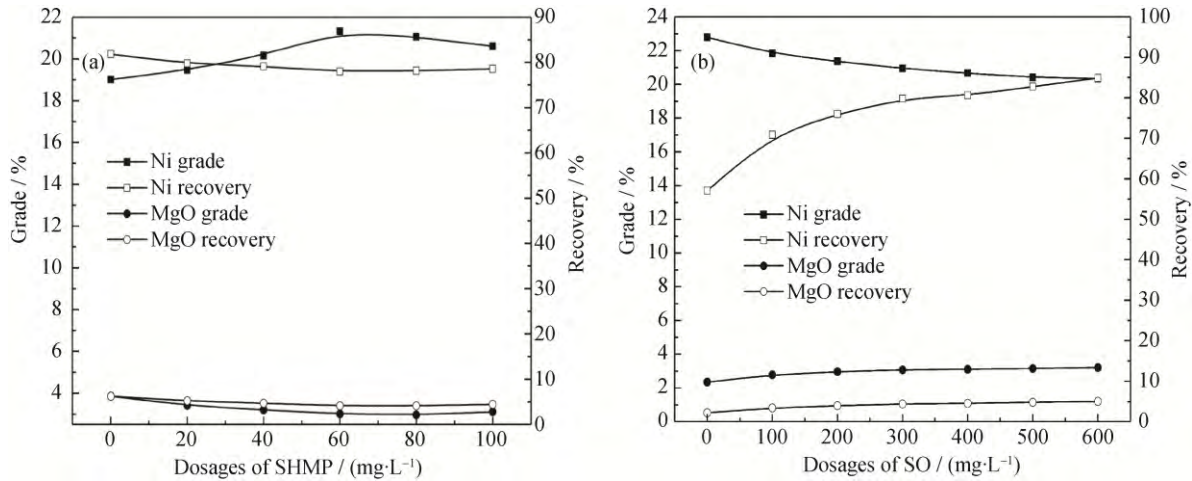
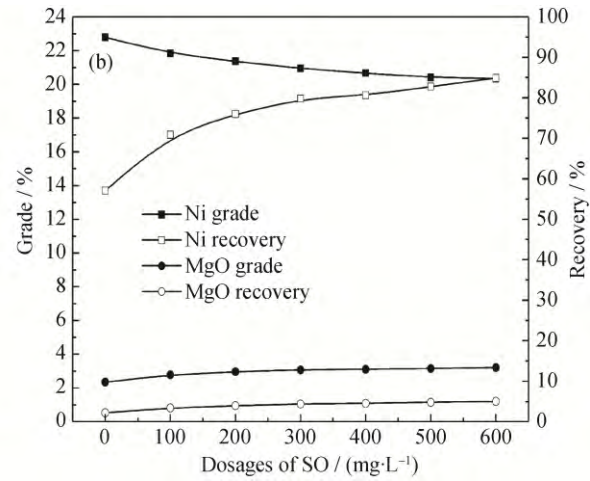


Fig. 6. Effects of SHMP (a, 200 mg·L⁻¹ SO) and SO (b, 60 mg·L⁻¹ SHMP) on magnetic coating behaviors of mixed minerals.

Fig. 7 depicts the effect of magnetic field intensity and stirring speed on the pentlandite–serpentine mixture separation, with the other parameters kept constant. Fig. 7(a) shows the effect of increasing the magnetic field intensity from 0.06 to 0.3 T on the grade and recovery of Ni and MgO. Apparently, when the magnetic field intensity increased from 0.06 to 0.25 T, the Ni grade of magnetic concentrate increased gradually from 20.6% to the maximum of 22.4%, and the recovery increased from 72.3% to the maximum of 85.3%. With further increase in the magnetic field intensity, for example to 0.3 T, the Ni recovery still increased while the Ni grade decreased. This is due to the slight physical entrapment of magnetic serpentine in the magnetite fines (leading to the decline of the Ni grade). Simultaneously, the pentlandite particles coated by small quantities of magnetite fines were also collected and thus

of Ni and MgO, the optimum dosage of SO was determined to be 400 mg·L⁻¹.



led to the increase in the Ni recovery. Compared with the Ni grade and recovery, the MgO grade and recovery increased steadily with increasing magnetic field intensities. The above results suggest that the magnetic field intensity of 0.25 T is satisfactory for the magnetic separation of pentlandite from serpentine. Fig. 7(b) illustrates that the separation efficiency of artificial minerals was influenced by the stirring speeds variation from 1500 to 2600 r·min⁻¹, and that the optimum stirring speed was 2300 r·min⁻¹ regarding the difference in Ni and MgO indexes of magnetic concentrate. When the stirring speed increased from 1500 to 2600 r·min⁻¹, the grade and recovery of MgO decreased gradually (Fig. 7(b)), and the grade reduced from 4.2% to about 2.8%. For the Ni grade and recovery, the grade rose significantly with increase in the stirring speed. This indicates that the magnetite fines may preferentially coat the

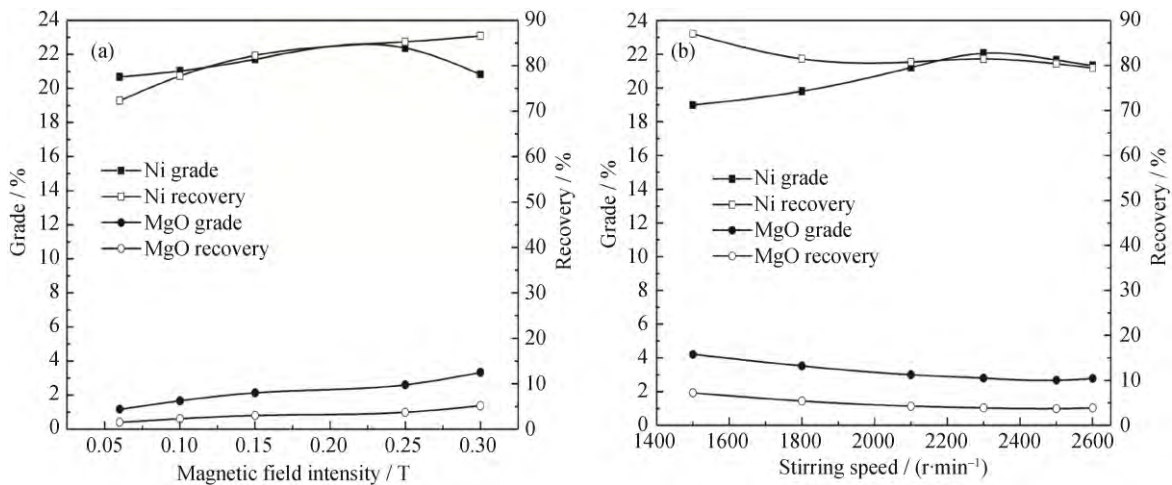


Fig. 7. Effects of magnetic field intensity (a) and stirring speed (b) on magnetic coating behaviors of mixed minerals.

pentlandite surfaces, which would continuously enhance the magnetism until the pentlandite particles are well separated from the serpentine particles by magnetic separation. With further increase in the stirring speed to over 2300 $\text{r}\cdot\text{min}^{-1}$, the Ni grade began to decrease because of the scattering or detaching of the magnetite-pentlandite aggregates by the strong agitation.

To further verify the feasibility of separating pentlandite from serpentine using the selective magnetic coating method, coating experiments were conducted using the mixed minerals under the following conditions: pH of 6.8–7.2, SHMP dosage of 60 $\text{mg}\cdot\text{L}^{-1}$, SO dosage of 400 $\text{mg}\cdot\text{L}^{-1}$, magnetic field intensity of 0.25 T, and stirring speed of 2300 $\text{r}\cdot\text{min}^{-1}$. The obtained results show that the Ni grade of the magnetic concentrate increased from 8.4% to 20.8%, with a Ni recovery of 80.5%, and the MgO content in the magnetic concentrate reduced to 4.2wt%, which was satisfactory for separating pentlandite from the mixed minerals containing serpentine using selective magnetic coating technology. Therefore, this technology may be applicable for sorting serpentine-bearing nickel sulfide ores and thus deserves further study.

3.3. FTIR analyses of minerals in the absence and presence of reagents and magnetite

To verify the above experimental results, an FTIR study was first conducted to investigate the possible interaction of reagents (SHMP and SO) with magnetite, serpentine, and pentlandite surfaces. The FTIR spectra of magnetite, serpentine, and pentlandite without and with the reagents are shown in Figs. 8–10.

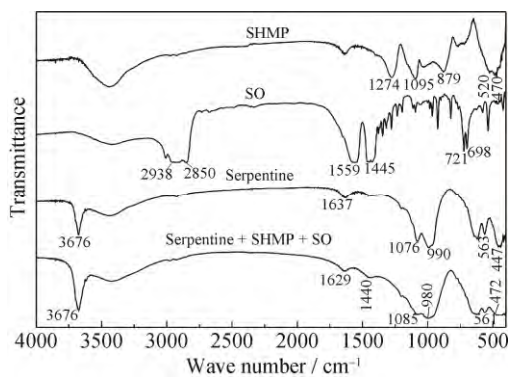


Fig. 8. FTIR spectra of serpentine without and with SHMP and SO.

The infrared spectra of SHMP and SO have been well studied by different scholars [14–17], and are as shown in Fig. 8. In the SHMP spectrum, the sharp peaks near 1274, 1095, and 879 cm^{-1} correspond to the stretching vibrations

of $\text{P}=\text{O}$, $\text{P}-\text{O}$, and $\text{P}-\text{O}-\text{P}$, respectively. The peaks at 520 and 470 cm^{-1} were due to the stretching vibration of $\text{P}-\text{O}$ from the phosphate group. In the SO spectrum, the unsaturated carboxylic acids with double bonds occurred in the range of 1690–1715 cm^{-1} , which were the peaks at 1559 and 1445 cm^{-1} . The peaks at 2938 and 2850 cm^{-1} were due to the stretching vibrations of methylene group and methyl group, respectively. The peaks at 721 and 698 cm^{-1} were due to $-\text{CH}_2$ stretching vibration. In the serpentine spectrum, the peaks at 3676 and 1637 cm^{-1} were both due to $-\text{OH}$ stretching vibration on $\text{Mg}-\text{OH}$ group. The peaks at 1076 and 990 cm^{-1} were due to $\text{Si}-\text{O}$ stretching vibration, and the peaks at 563 and 447 cm^{-1} were due to the flexural vibrations of $\text{Mg}-\text{O}$ [18].

Compared with the spectrum of serpentine untreated with reagents, the spectrum of serpentine treated with SHMP and SO did not show significant changes besides the presence of a new weak peak at 1440 cm^{-1} , inferring the occurrence of weak molecular adsorption to a certain extent [19]. In addition, other peaks also shifted slightly, which infers that SO was slightly adsorbed on serpentine, resulting in the coating of small magnetite fines on the serpentine surfaces and the increase of the MgO content in the magnetic concentrate, which is consistent with the previous coating experiments.

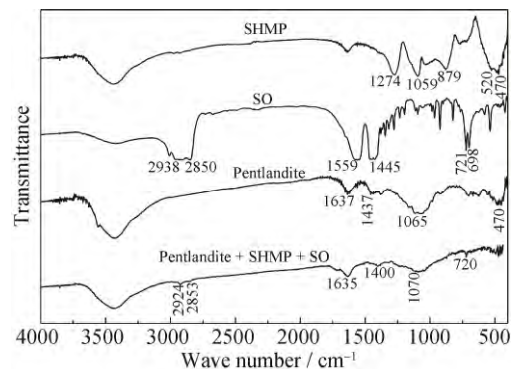


Fig. 9. FTIR spectra of pentlandite without and with SHMP and SO.

Fig. 9 presents the spectra of pentlandite untreated and treated with SHMP and SO. The sharp peaks at 1065 and 470 cm^{-1} were due to $\text{S}=\text{S}$ stretching vibration and $\text{Ni}-\text{S}$ or $\text{Fe}-\text{S}$ stretching vibration, respectively, which were the unique and distinguishing characteristic of pentlandite [20]. The peak of 1437 cm^{-1} was due to $\text{Fe}-\text{SO}$ stretching vibration, attributed to the oxidation of the pentlandite surfaces; this was beneficial to the adsorption of SO on the pentlandite surfaces [21]. After the pentlandite interacted with SHMP and SO, obvious new adsorption peaks emerged at 2924 and 2853 cm^{-1} , respectively, which is attributed to the

stretching vibration of $-\text{CH}_2$ in SO, but the adsorption intensities were weak, indicating that physical adsorption possibly occurred on the pentlandite surfaces [22]. Other peaks of original pentlandite present at 1437 cm^{-1} shifted to 1400 cm^{-1} ; this is attributed to the stretching vibration of $\text{C}=\text{O}$ in SO [23–24]. This proves that physical adsorption or molecular adsorption of SO occurred with SO absorption on pentlandite surfaces. Thus, the adsorption of SO on the pentlandite surfaces would favor the coating of magnetite fines on the pentlandite surfaces.

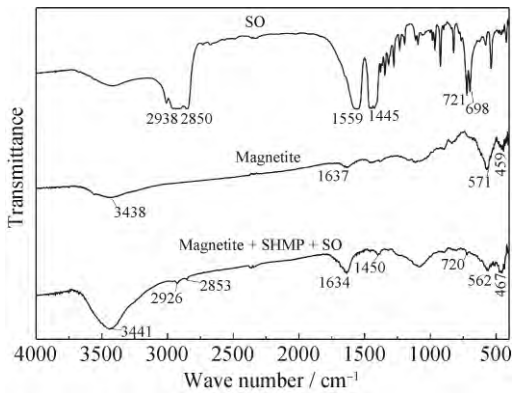


Fig. 10. FTIR spectra of magnetite without and with SHMP and SO.

Fig. 10 shows that the characteristic peaks of magnetite appeared around 459 and 571 cm^{-1} ; this is due to $\text{Fe}-\text{O}$ bonding [18]. Other peaks around 3438 and 1637 cm^{-1} correspond to the stretching vibration of OH groups and bending vibration of water molecules, respectively, indicating the presence of OH groups or water molecule in magnetite [25]. When the magnetite interacted with SHMP and SO, the characteristic magnetite peaks of 459 and 571 cm^{-1} shifted to 467 and 562 cm^{-1} , respectively. The OH stretching vibration was shifted by only 3 cm^{-1} , but its intensity was strengthened, indicating the involvement of OH groups in the adsorption on magnetite. In addition to the above changes, some new peaks were observed around 2926 , 2853 and 1450 cm^{-1} ; this is due to $-\text{CH}_2$ and $-\text{COOH}$ stretching vibrations, representing the adsorption of SO molecules and ions on the magnetite particles [26–27]. Therefore, quantities of magnetite fines could coat the pentlandite surfaces and enhance its magnetism, so that the pentlandite can be recovered from serpentine through magnetic separation.

Fig. 11 shows the spectrum of magnetic concentrates. Compared with the spectra of pentlandite and magnetite, an obvious new sharp peak of $\text{Fe}-\text{O}$ emerged near 563 cm^{-1} , and a strong adsorption peak emerged near 475 cm^{-1} ; this

indicates the occurrence of magnetic coating of magnetite on the pentlandite surfaces. Direct evidences were also provided by the SEM observation and XRD pattern.

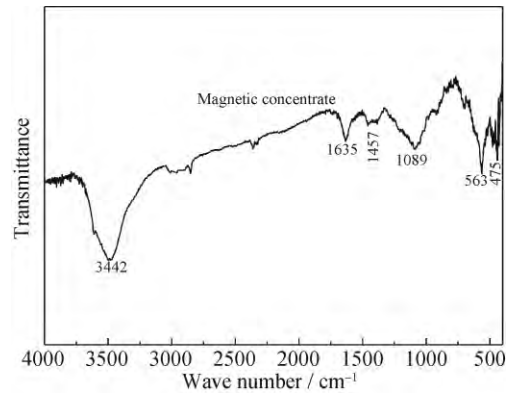


Fig. 11. FTIR spectra of magnetic concentrate.

3.4. XRD and SEM studies of minerals after magnetic coating

To further verify the above experimental results, the magnetic concentrates were collected for XRD and SEM-EDS analyses. As shown in Fig. 12(a), the XRD analysis indicates pentlandite as the main phase with minor pyrite. Furthermore, the characteristic peak of magnetite was easily observed in the concentrates after magnetic coating, which demonstrates the occurrence of magnetic coating on the pentlandite surface.

From the micrograph of the magnetic concentrate (Fig. 12(b)), it can be deduced that the pentlandite surface was extensively covered with many small particle fines, and the EDS analyses (Figs. 12(c) and 12(d)) further confirm that magnetite fines were present on the pentlandite surface, indicating the formation of selective magnetic coating on the surface: for the coating particles (1), Fe and O were obvious, indicating the presence of magnetite, while the coated particle (2) consisted of Ni, Fe, S and O (because the oxidation of pentlandite surfaces) indicating the presence of the pentlandite. Therefore, the SEM image and EDS patterns also prove that the pentlandite surfaces were coated by the magnetite fines.

3.5. Interactions of magnetite with pentlandite and serpentine in the presence of reagents

The interactions between magnetite fractions with pentlandite and serpentine particles in the presence of SHMP and SO at the natural pH were calculated by DLVO theory, as shown in Figs. 13 and 14. The DLVO calculation in the pentlandite-serpentine system has been described in detail in our previous study [8].

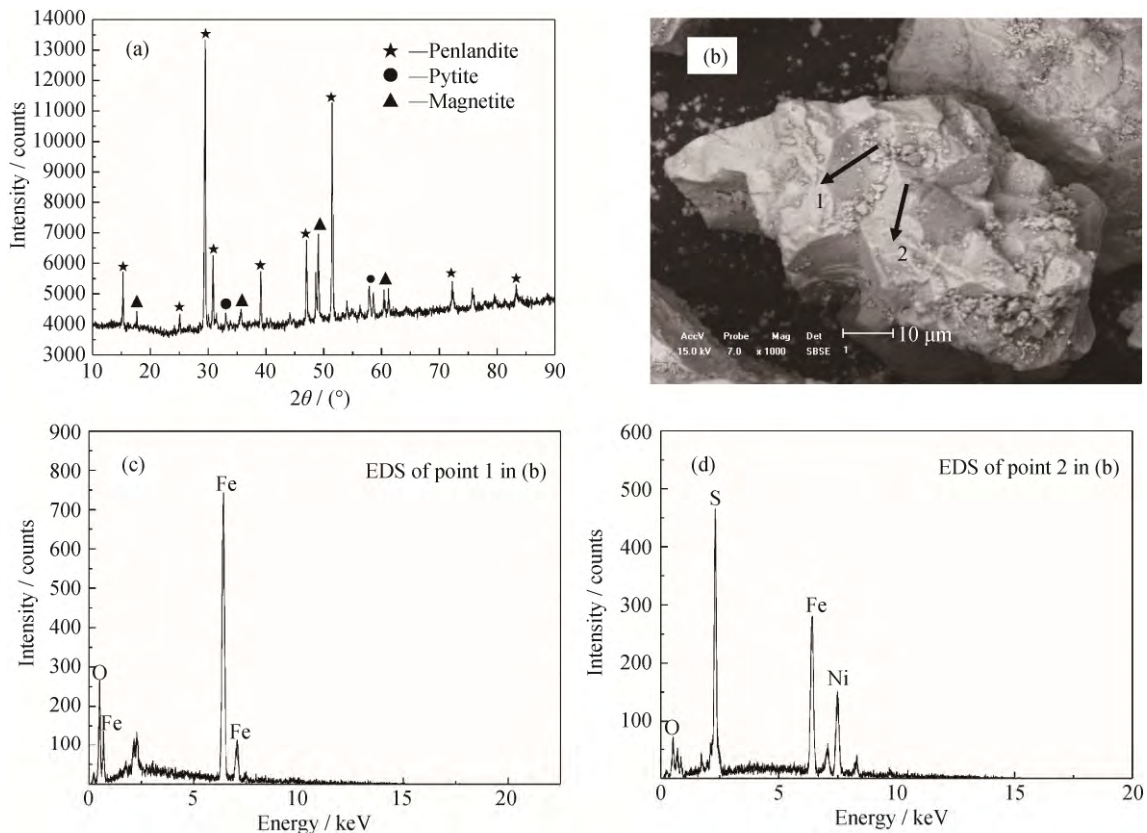


Fig. 12. XRD pattern (a) and SEM image (b) of magnetic concentrate and EDS patterns (c, d) of the coating and coated particles.

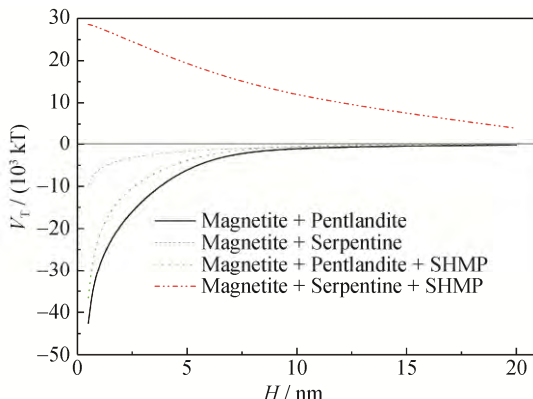


Fig. 13. Interactions of magnetite with pentlandite and serpentine in absence and presence of SHMP (V_T is the total interaction; H is the distance between two particles).

The attractive interactions of magnetite-pentlandite and magnetite-serpentine were observed without addition of SHMP, and the interaction of magnetite-serpentine was weaker than that of magnetite-pentlandite (Fig. 13). After SHMP was added, the attractions of the two interactions decreased. The attractive magnetite-serpentine interaction became strongly repulsive, whereas the magnetite-pentlandite attraction was still strong, which favored the coating of magnetite on the pentlandite particles rather than the serp-

entine, resulting in selective magnetic coating on the pentlandite surfaces. This is consistent with the above magnetic coating tests. Therefore, the addition of SHMP is necessary for the selective magnetic coating in the pentlandite-serpentine system.

The results of FTIR spectra indicate that the SO coagulant was mainly absorbed on the pentlandite and magnetite surfaces. Therefore, a hydrophobic interaction must exist between them, in addition to the van der Waals and electrical interactions. The hydrophobic interaction (V_{HPB}) comes from the perturbation of the water structure as the mineral particles approach each other [13]. The interaction is usually within relatively short range of 0–20 nm and is much stronger than the van der Waals and electrical interactions. For two spherical particles, with the adsorbed layer thicknesses δ , the hydrophobic interaction is expressed in the following form [28]:

$$V_{HPB} = -\frac{C_{HPB}(R_1 + \delta)(R_2 + \delta)}{(R_1 + \delta) + (R_2 + \delta)} l_{HPB} \exp\left(-\frac{H - 2\delta}{l_{HPB}}\right) \quad (1)$$

where V_{HPB} is the hydrophobic interaction, kT ; C_{HPB} is the hydrophobic interaction constant, $N \cdot m^{-1}$; δ is the adsorbed layer thickness on mineral particles, m ; l_{HPB} is the hydrophobic interaction decay length, m ; R is the radius of spher-

ical particles, m ; and H is the distance between two mineral particles, m .

For calculation purposes, the following assumptions have been made. The SO adsorbed on the pentlandite and magnetite is the monomolecular adsorption layer, and hence, the C_{HPB} , l_{HPB} , and δ values are $0.14 \text{ N} \cdot \text{m}^{-1}$, 1.05 nm , and 1.3 nm , respectively. The hydrophobic interaction was calculated according to Eq. (1). The interaction curve of magnetite-pentlandite particles with SHMP and SO at the natural pH is shown in Fig. 14.

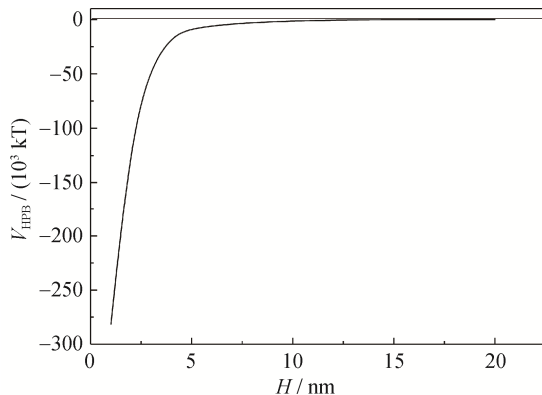


Fig. 14. Hydrophobic interactions between magnetite and pentlandite in presence of SHMP and SO.

Comparing the interaction shown in Fig. 14 with that in Fig. 13, the hydrophobic interaction between magnetite and pentlandite particles was very strong after the addition of SHMP and SO. The approximate distance in the net attractive interaction occurred at 10 nm for the magnetite-pentlandite interaction. The closer the two particles, the stronger the attractive interaction between them; therefore, pentlandite particles were strongly coated by the fine magnetite particles under the hydrophobic interaction. This observation was completely proved by magnetic coating-magnetic separation tests (Fig. 6). Hence, based on the above results, the driving force for the selective magnetic coating of magnetite on the pentlandite particles seems to be the hydrophobic interaction when surfactants were used in the pentlandite-serpentine system.

4. Conclusions

In this study, the factors and mechanisms, such as pH and SHMP and SO reagents, affecting the magnetic coating of magnetite on the separation of pentlandite from serpentine were studied in detail. The major conclusions are as follows:

(1) The optimal conditions of selective magnetic coating were revealed as follows: pH of $6.8\text{--}7.2$, stirring speed of $2300 \text{ r} \cdot \text{min}^{-1}$, magnetic field intensity of 0.25 T , SHMP of

$60 \text{ mg} \cdot \text{L}^{-1}$, and SO of $400 \text{ mg} \cdot \text{L}^{-1}$. Thus, the Ni grade of magnetic concentrate increased from 8.4% to 20.8% , with a Ni recovery of 80.5% , and the MgO content in the magnetic concentrate reduced to $4.2\text{wt}\%$.

(2) The results of FTIR spectra indicated that SO could be both selectively and strongly adsorbed on the pentlandite and magnetite surfaces, while a weak SO adsorption occurred on the serpentine surface due to the restraint of SHMP. Therefore, SHMP and SO surfactants are necessary for the selective magnetic coating in the pentlandite-serpentine system.

(3) After adding SHMP, the attractive magnetite-serpentine interaction turned strongly repulsive. When SO was added, a significant hydrophobic interaction occurred between the hydrophobic particles of pentlandite and magnetite, which significantly contributed to the selective magnetic coating. Thus, the target mineral of pentlandite was strongly coated by magnetite particles, and then, the magnetite-pentlandite aggregates were successfully separated by magnetic separation.

Acknowledgements

This work was financially supported by the National Natural Science Foundation of China (No. 51704057), the China Postdoctoral Science Foundation (No. 2017M621153), the Postdoctoral Science Foundation of Northeastern University (No. 20170312), the Fundamental Research Funds for the Central Universities (No. N170104018), and the Open Fund Project of Shaanxi Key Laboratory of Comprehensive Utilization of Tailings Resources, China (No. 2017SKY-WK012).

References

- [1] J. Cao, X.Q. Hu, Y.C. Luo, L. Qi, G.Q. Xu, and P.F. Xu, The role of some special ions in the flotation separation of pentlandite from lizardite, *Colloids Surf. A*, 490(2016), p. 173.
- [2] B. Feng, Q.M. Feng, and Y.P. Lu, A novel method to limit the detrimental effect of serpentine on the flotation of pentlandite, *Int. J. Miner. Process.*, 114-117(2012), p. 11.
- [3] A.M. Kusuma, Q.X. Liu, and H.B. Zeng, Understanding interaction mechanisms between pentlandite and gangue minerals by zeta potential and surface force measurements, *Miner. Eng.*, 69(2014), p. 15.
- [4] M. Alvarez-Silva, A. Uribe-Salas, K.E. Waters, and J.A. Finch, Zeta potential study of pentlandite in the presence of serpentine and dissolved mineral species, *Miner. Eng.*, 85(2016), p. 66.
- [5] P. Parsonage, Principles of mineral separation by selective magnetic coating, *Int. J. Miner. Process.*, 24(1988), No. 3-4,

p. 269.

[6] S. Singh, H. Sahoo, S.S. Rath, A.K. Sahu, and B. Das, Recovery of iron minerals from Indian iron ore slimes using colloidal magnetic coating, *Powder Technol.*, 269(2015), p. 38.

[7] Y. Ucbras, V. Bozkurt, K. Bilir, and H. Ipek, Concentration of chromite by means of magnetic carrier using sodium oleate and other reagents, *Physicochem. Prob. Miner. Process.*, 50(2014), No. 2, p. 767.

[8] J.W. Lu, Z.T. Yuan, J.T. Liu, L.X. Li, and S. Zhu, Effects of magnetite on magnetic coating behavior in pentlandite and serpentine system, *Miner. Eng.*, 72(2015), p. 115.

[9] L.H. Xu, H.Q. Wu, F.Q. Dong, L. Wang, Z. Wang, and J.H. Xiao, Flotation and adsorption of mixed cationic/anionic collectors on muscovite mica, *Miner. Eng.*, 41(2013), p. 41.

[10] X.M. Luo, W.Z. Yin, C.Y. Sun, N.L. Wang, Y.Q. Ma, and Y.F. Wang, Improved flotation performance of hematite fines using citric acid as a dispersant, *Int. J. Miner. Metall. Mater.*, 23(2016), No. 10, p. 1119.

[11] D. Li, W.Z. Yin, J.W. Xue, J. Yao, Y.F. Fu, and Q. Liu, Solution chemistry of carbonate minerals and its effects on the flotation of hematite with sodium oleate, *Int. J. Miner. Metall. Mater.*, 24(2017), No. 7, p. 736.

[12] Z.T. Yuan, J.W. Lu, J.T. Liu, L.X. Li, and S.Y. Wang, Enhancement of pentlandite surface magnetism and implications for its separation from serpentine via magnetic separation, *Trans. Nonferrous Met. Soc. China*, 27(2017), No. 1, p. 204.

[13] G.N. Anastassakis, Separation of fine mineral particles by selective magnetic coating, *J. Colloid Interface Sci.*, 256(2002), No. 1, p. 114.

[14] Y.P. Lu, M.Q. Zhang, Q.M. Feng, T. Long, L.M. Ou, and G.F. Zhang, Effect of sodium hexametaphosphate on separation of serpentine from pyrite, *Trans. Nonferrous Met. Soc. China*, 21(2011), No. 1, p. 208.

[15] W.J. Liu, J. Zhang, W.Q. Wang, J. Deng, B.Y. Chen, W. Yan, S.Q. Xiong, Y. Huang, and J. Liu, Flotation behaviors of ilmenite, titanite, and forsterite using sodium oleate as the collector, *Miner. Eng.*, 72(2015), p. 1.

[16] J. Tian, L.H. Xu, W. Deng, H. Jiang, Z.Y. Gao, and Y.H. Hu, Adsorption mechanism of new mixed anionic/cationic collectors in a spodumene-feldspar flotation system, *Chem. Eng. J.*, 164 (2017), p. 99.

[17] Y.S. Gao, Z.Y. Gao, W. Sun, Z.G. Yin, J.J. Wang, and Y.H. Hu, Adsorption of a novel reagent scheme on scheelite and calcite causing an effective flotation separation, *J. Colloid Interface Sci.*, 512 (2018), p. 39.

[18] L. Wen, *Infrared Spectroscopy of Mineral*, Chongqing University Press, Chongqing, 1989, p. 45.

[19] D.Z. Wang, *Flotation Reagent: Fundamentals and Application*, Metallurgical Industry Press, Beijing, 1982.

[20] Q.M. Feng, G.F. Zhang, and Y.P. Lu, Mechanism and collection behavior of a new collector BS-4 on blucite, *J. Cent. South Univ. Technol.*, 30(1999), No. 3, p. 27.

[21] K.L. Zhao, G.H. Gu, C.L. Wang, X.Y. Rao, X.H. Wang, and X.X. Xiong, The effect of a new polysaccharide on the depression of talc and the flotation of a nickel copper sulfide ore, *Miner. Eng.*, 77(2015), p. 99.

[22] J.G. Zhu and Y.S. Zhu, *Chemical Principles of Flotation Reagent*, Central South University of Technology Press, Changsha, 1996.

[23] L.H. Xu, J. Tian, H.Q. Wu, W. Deng, Y.H. Yang, W. Sun, Z.Y. Gao, and Y.H. Hu, New insights into the oleate flotation response of feldspar particles of different sizes: Anisotropic adsorption model, *J. Colloid Interface Sci.*, 505(2017), p. 500.

[24] J. Tian, L.H. Xu, H.Q. Wu, S. Fang, W. Deng, T.F. Peng, W. Sun, and Y.H. Hu, A novel approach for flotation recovery of spodumene, mica and feldspar from a lithium pegmatite ore, *J. Clean. Prod.*, 174 (2018), p. 625.

[25] B. Kar, H. Sahoo, S.S. Rath, and B. Das, Investigations on different starches as depressants for iron ore flotation, *Miner. Eng.*, 49(2013), p. 1.

[26] C. Magnet, C. Lomenech, C. Hurel, P. Reilhac, F. Giulieri, A.M. Chaze, J. Persello, and P. Kuzhir, Adsorption of nickel ions by oleate-modified magnetic iron oxide nanoparticles, *Environ. Sci. Pollut. Res.*, 24(2017), No. 8, p. 7423.

[27] P. Roonasi, X.F. Yang, and A. Holmgren, Competition between sodium oleate and sodium silicate for a silicate/oleate modified magnetite surface studied by *in situ* ATR-FTIR spectroscopy, *J. Colloid Interface Sci.*, 343(2010), No. 2, p. 546.

[28] S.C. Lu, *Industrial Suspensions: Properties, Preparation and Processing*, Chemical Industry Press, Beijing, 2003, p. 598.